Taylor & Francis
Taylor & Francis Group

ORIGINAL RESEARCH

🔓 OPEN ACCESS | Check for updates

Suppression of prostate cancer and amelioration of the immunosuppressive tumor microenvironment through selective immunoproteasome inhibition

Julia Koerner [ID][a], Dennis Horvath [ID][a,b], Franziska Oliveri [ID][a], Jun Li [ID][c], and Michael Basler [ID][a,d]

[a]Division of Immunology, Department of Biology, University of Konstanz, Konstanz, Germany; [b]Centre for the Advanced Study of Collective Behaviour, University of Konstanz, Konstanz, Germany; [c]Department of Urologic Oncology Surgery, Chongqing University Cancer Hospital, Chongqing, China; [d]Biotechnology Institute Thurgau (BITg) at the University of Konstanz, Kreuzlingen, Switzerland

ABSTRACT

New treatment options to battle hormone-refractory prostate carcinoma (PC) are a pressing medical need. Chronic inflammation has been implicated in PC etiology. The pro-inflammatory cytokines IL-6, IL-23 and IL-17 are key mediators to promote growth of PC. Here, we evaluate the potential of immunoproteasome inhibition for anti-inflammatory and direct anti-tumorigenic therapy of PC. The anti-tumor effect of immunoproteasome inhibitor ONX 0914 was tested in mouse and human PC cells and the *in vivo* therapeutic efficacy of immunoproteasome inhibition was analyzed in transgenic adenocarcinoma of the mouse prostate (TRAMP) mice in preventive and therapeutic settings and in castration-resistant (CR) PC after castration. Inhibition of the immunoproteasome subunit LMP7 induced apoptotic cell death in PC cell lines. In TRAMP mice, ONX 0914-treatment resulted in significant inhibition of PC growth with a decreased frequency of malignant prostatic lesions and inhibition of metastasis formation. The number of immunosuppressive myeloid cells in PC was greatly reduced in response to ONX 0914. Thus, immunoproteasome inhibition shows remarkable efficacy against PC progression *in vivo* and impedes tumor recurrence in CRPC-TRAMP mice by blocking the immunosuppressive inflammatory response in the tumor microenvironment. In conclusion, we show that the immunoproteasome is a promising drug target for the treatment of PC.

Introduction

Prostate cancer (PC) is the second most frequent malignant disease of men and the sixth leading cause of cancer-related deaths worldwide. Besides radical prostatectomy or radiation therapy, androgen deprivation therapy (ADT) is a standard treatment option for androgen-sensitive PC, such as high-risk localized PC, recurrent, progressive or metastatic PC. Surgical or pharmacological androgen ablation with recently approved second-generation drugs like enza lutamide or bica-lutamide initially arrests tumor growth, but eventually almost all PC patients will progress to hormone refractory PC with a median overall survival of 13–32 months and a 15% 5-year survival rate.

Multiple epidemiological and histopathological studies have shown the involvement of inflammation in cancer progression and development. Almost all surgical PC specimens exhibit a pro-inflammatory profile associated with reactive nitrogen and oxygen radicals and show dysfunctional cellular immunity with a high abundance of immunosuppressive cells.[1] Chronic inflammation is implicated in the development of prostatic intraepithelial neoplasia and carcinoma.[2] The pro-inflammatory signaling evokes proliferative inflammatory atrophy, which is a precursor lesion to prostatic intraepithelial neoplasia (PIN). Especially, tumor promoting T helper 17 (Th17) cells and pro-inflammatory IL-17 signaling stimulate prostate tumor growth by supporting tumor cell survival and proliferation.[3] IL-17 signaling results in activation of the NF-κB pathway that culminates in transcription of various pro-inflammatory mediators, including IL-6. These factors promote tumorigenesis by increased proliferation, attenuated apoptosis and sustained angiogenesis, as well as the creation of an immunotolerant microenvironment. Reduced tumor formation and decreased numbers of invasive prostate adenocarcinomas were achieved by IL-17 abrogation in several studies employing *Pten* conditional knockout mice.[3,4] The frequency of Th17 cells is increased in human PC tissue which correlates with worse clinical outcome.[5,6] Additionally, the prostate tumor microenvironment (TME) is coined by upregulation of pro-inflammatory cytokines that induced increased infiltration of immunosuppressive myeloid-derived suppressor cells (MDSC) and tumor-associated macrophages (TAM).[7] The enhanced myeloid compartment in human PC specimen was concomitant with reduced overall survival and decreased sensitivity to different chemotherapeutic options[8] MDSC in PC tissue secrete pro-tumorigenic IL-23, which stabilizes a Th17-dependent transcriptional profile and activates downstream androgen receptor (AR) target genes, thus promoting tumor cell survival and proliferation in the absence of androgens.[9]

The 26S proteasome is the major multicatalytic endoprotease and responsible for the degradation of regulatory as well as misfolded intracellular proteins.[10] The active sites are located within the proteolytic core complex which consists of 28 subunits arranged into four stacked rings consisting of α- and β-subunits. Three different subunits (β1, β2, and β5) exhibit different peptidase activities of the proteasome. Stimulation of cells with pro-inflammatory cytokines such as IFNγ or TNF in inflamed tissue leads to incorporation of the inducible proteolytically active subunits low molecular mass peptide 2 (LMP2, β1i), multicatalytic endopeptidase complex-like (MECL)-1 (β2i), and LMP7 (β5i), thereby forming the immunoproteasome, which is also constitutively expressed in immune cells.[11] The altered cleavage pattern of the immunoproteasome shapes the antigenic repertoire of MHC class I bound T cell epitopes at sites of inflammation resulting in efficient activation of cytotoxic T lymphocytes (CTLs).[12] In the past, we have shown that the immunoproteasome has additional functions such as influencing cytokine production and T helper cell differentiation, as well as T cell survival, especially in the pathogenesis of autoimmune diseases. Immunoproteasome inhibition using the LMP2/7-selective inhibitor ONX 0914 (formerly called PR-957) was shown to modulate cytokine production, leading to amelioration of clinical symptoms in multiple mouse models of autoimmune diseases, such as rheumatoid arthritis,[11] experimental autoimmune encephalomyelitis (EAE)[13] or dextran sodium sulfate (DSS)-induced experimental colitis.[14] ONX 0914 treatment achieved suppressed production of pro-inflammatory cytokines IL-23, TNF and IL-6, and reduced Th17 responses[15,16] resulting in a suppressed inflammatory environment. Recently, we and others discovered the therapeutic effect of ONX 0914 treatment on colon cancer development in chemically induced and transgenic mouse models.[17,18] These results suggest ONX 0914 treatment as a promising therapeutic intervention with inflammation-associated cancer. Due to tumor-elicited inflammation observed in clinical samples and mouse models of PC[19] it was pertinent to analyze immunomodulatory properties and potential direct tumoricidal effects of ONX 0914 also in this disease entity. Although selective immunoproteasome inhibitors have been reported to exhibit anti-proliferative, pro-apoptotic, and anti-angiogenic effects in different cells and tumor models, their effect on malignant progression and metastasis of PC has not been tested *in vivo*. This study reveals pro-apoptotic effects of ONX 0914 in murine and human PC cell lines, as well as remarkable therapeutic efficacy against PC and CRPC in an autochthonous mouse model of PC *in vivo*.

Materials and methods

Cell lines

Human PC cell lines LNCaP, DU-145 and PC3 were originally purchased from ATCC and maintained in RPMI-1640 medium supplemented with GlutaMAX, 10% FCS, and 100 U/ml penicillin/100 μg/ml streptomycin. The mouse PC cell line TRAMP-C2 was cultured in DMEM (w/o pyruvate), complemented with GlutaMAX, 5% FCS, 5% Nu-serum, 5 μg/ml insulin, 10^{-8} M 5α-dihydrotestosterone (DHT) and 100 U/ml penicillin/100 μg/ml streptomycin. Cell cultures were maintained at 37°C with 5% CO_2 in a humidified atmosphere. Adherent cells were detached by incubation with 0.05% trypsin-EDTA for 5 minutes at 37°C. Cell lines were routinely tested for mycoplasma by service provision at Microsynth AG, Switzerland.

Animals and ethics statement

TRAMP mice[20] and C57BL/6 mice were originally purchased from Jackson Laboratories. $LMP7^{-/-}$ mice[21] were kindly provided by Dr. John J. Monaco (Department of Molecular Genetics, Cincinnati Medical Center, OH). Male TRAMP mice were generated by mating hemizygous female TRAMP mice with male C57BL/6 mice. Transgenic animals were verified via PCR using genomic DNA extracted from ear biopsies, as previously described.[22] Animals were further bred in the air-conditioned animal facility of the University of Konstanz or the Chongqing University Cancer Hospital under specific pathogen-free conditions with a 12-hour light/dark cycle and lights on at 7 a.m. Animals were provided *ad libitum* access to standard, autoclaved laboratory animal diet and water. Mice were randomly assigned into groups and sacrificed after 32 or 50 weeks or until adverse symptoms appeared or large abdominal tumors were detected by palpation. Animal experiments have been approved by the Ethics Committee of Chongqing University Cancer Hospital (CZLS2020289-A) or the Review Board of Governmental Presidium Freiburg (T-19/04TFA).

Generation of murine MDSC and TAMs *in vitro*

Cells from proliferating mouse bone marrow progenitors were isolated from femur and tibia of C57BL/6 mice and differentiated as previously described.[23] Murine MDSC were generated by culturing 3×10^6 unfractionated bone marrow cells in complete medium containing 40 ng/mL GM-CSF (Peprotech) and 40 ng/mL IL-6 (Biolegend) in 10 cm dishes. Tumor-associated macrophages were generated by culturing 3×10^6 unfractionated bone marrow cells with 30 ng/mL M-CSF (Biolegend) in 10 cm dishes. The same amount of cytokines were additionally added on day 2. Cells were harvested on day 4 after detaching with 5 mM EDTA/PBS for 20 minutes at 37°C.

Flow cytometry

Single-cell suspensions from tumors were generated using the mouse tumor dissociation kit with the gentleMACS Octo Dissociator according to the manufacturer's protocol (Miltenyi Biotec). Cells were labeled with fluorochrome-conjugated antibodies for 30 min at 4°C. Live/Dead cell discrimination was performed by addition of Zombie Fixable Viability™ Dyes (BioLegend). For intracellular staining, cells were fixed and permeabilized using a Cytofix/Cytoperm Kit (BD Biosciences) according to the manufacturer's instructions as preparation for intracellular staining using fluorescently labeled antibodies in BD Perm/Wash™ buffer (BD Biosciences). Antibody staining was performed in the presence

of purified 2.4G2 antibody (Fc block). Apoptotic cells were detected using the FITC Annexin V Apoptosis Detection Kit with PI (Biolegend) according to the manufacturer's instructions. Antibodies for flow cytometry were purchased from either BD Biosciences, Invitrogen, or BioLegend. Flow cytometry was performed using BD LSRFortessa™ or BD FACSLyric™ instruments (BD Biosciences). A list of flow cytometry antibodies is available in the Supplementary Information. Data were analyzed using FlowJo software (Tree Star, Inc., Version 10).

Immunoproteasome inhibition in vitro and in vivo

ONX 0914[11] was generously provided by Dr Christopher J. Kirk (Kezar Life Sciences). For inhibition in vitro, a 10 mM stock solution of ONX 0914 in DMSO was prepared and stored at −80°C. A total concentration of 300 nM in DMSO was added into the cell culture medium. The equal amount of DMSO was used as vehicle control. For in vivo studies, ONX 0914 was formulated in an aqueous solution of 10% (w/v) sulfobutyl-lether-ß-cyclodextrin and 10 mM sodium citrate (pH 6). 10 mg/kg of the inhibitor was administered subcutaneously in a volume of 100 μl, control mice received 100 μl vehicle only.

TRAMP prostate tumor model

Mice were s.c. treated with vehicle or ONX 0914 at a respective dose of 10 mg/kg three times a week. Mice were monitored for clinical signs of illness, especially abdominal tumors. Surgical castration was performed under isoflurane anesthesia at 24 weeks of age. Bilateral testes were removed through a scrotal midline incision by cauterizing the ductus deferens. The incision was closed by sterile suture. Longitudinal inhibitor treatment was started 4 weeks after castration as described above. PC-related mortality and euthanasia were assessed as described above, 26 weeks after castration.

Histology and immunohistochemistry (IHC)

The lower genitourinary tract (GU), including seminal vesicles and prostate anterior and ventral lobes, was removed and weighed. Additionally, liver and lung were dissected and examined for macroscopic lesions. Organ tissue was immediately immersed into 10% neutral buffered formalin for 24 hours. Tissues were embedded as paraffin blocks and sectioned at 4 μm for Mayer's hematoxylin and eosin (H&E) staining and immunohistochemical staining using primary antibodies (as listed in the Supplementary Information). Morphological classification of prostatic lesions was assessed according to grading systems previously described:[24,25] healthy tissue, low- (LGPIN) or high-grade prostatic intraepithelial neoplasia (HGPIN), and well (WAC), or poorly differentiated adenocarcinoma (PAC). For IHC, sodium 0.1 mM citrate (pH 6) was applied for heat-induced antigen retrieval. Quenching was performed with 10% hydrogen-peroxide and 5% goat-serum in 0.1% PBS/Tween was used for blocking at RT for 1 hour. Primary antibody staining was performed by overnight incubation at 4°C. After that, HRP-conjugated secondary antibodies were applied for 2 hours at

RT. Slides were stained with an avidin-biotin-based peroxidase system. Positive immunoreactions were visualized using peroxidase substrate kits (ImmPACT®, Vector Laboratories) and counterstaining with hematoxylin or nuclear fast red (Vector Laboratories). Terminal deoxynucleotidyl transferase-mediated dUTP nick-end labeling (TUNEL) assay was performed using the Click-iT™ TUNEL Colorimetric IHC Detection Kit (Invitrogen) according to the manufacturer's instructions. Microscopy images of at least five random fields per sections were acquired using AxioVision (Rel. 4.8) software at the Axioplan 2 light microscope (Zeiss) and analyzed in a blinded manner.

Western blot analysis

Cells were lysed in RIPA buffer (50 mM Tris-buffered HCl, pH 7.5 containing 150 mM NaCl, 1% NP-40, 0.5% SDS) and tissue fractions were lysed in RIPA buffer supplemented with 2 mM Na_3VO_4, 10 mM NaF, 1 mM PMSF and complete protease inhibitor cocktail (Roche Pharmaceuticals) for 30 minutes on ice. Total protein in the supernatants of the cell extracts was quantified by the bicinchoninc acid method (Pierce BCA Protein Assay Kit, Thermo Scientific). Equal amounts of protein lysates (25 μg) were resolved under reducing conditions on 15% SDS-polyacrylamide gels for electrophoresis and transferred onto nitrocellulose-FL membranes (0.45 μm) (GE healthcare). Membranes were blocked in Odysee® blocking buffer (LI-COR Biosciences) for 1 h at RT and incubated using primary antibody in 1x Roti®-Block/TBS-T followed by fluorescently labeled IRDye® secondary anti-rabbit or anti-mouse Ig antibody (IRDye® 680, IRDye® 800, LI-COR Biosciences). A list of Western Blot antibodies can be found in the Supplementary Information. Protein bands were detected by NIR fluorescence using the Odyssey® Fc Infrared Imaging system (LI-COR Biosciences). Quantification of band intensities was performed with the aid of the Image Studio Lite software (LI-COR, Biosciences). To ascertain equivalent loading of the lanes and to normalize respective protein levels to internal loading controls, β-actin (1:5000, Cell Signaling) was used.

Data and code availability

All relevant data supporting the findings of this study are included within the article and supplementary information files or are available from the authors upon reasonable request.

Statistical analysis

Statistical significance was determined by applying two-tailed Student's t-test, one-way or two-way ANOVA analysis of variances followed by Bonferroni post hoc test or Tukey test for comparison of multiple groups. Dunnett's multiple comparison test was run if F achieved P < .05. The Kaplan-Meier method was used to estimate statistical significance in overall survival distribution between the groups. Unless noted in figure legends, data from at least three experiments or experiments using n ≥ 3 are presented as means ± SD. Statistical analyses were performed using GraphPad Prism Software

(version 9.1; GraphPad Software, Inc.). Statistical significance was achieved when $P < .05$. *$P < .05$; **$P < .01$; ***$P < .001$.

Results

The selective immunoproteasome inhibitor ONX 0914 causes proteostasis failure and apoptosis in prostate cancer cells

To selectively target immunoproteasome subunits *in vivo*, we first analyzed proteasome subunit composition in TRAMP prostate tissue. Immunoproteasome subunits are highly expressed in different lobes of TRAMP prostates (Figure 1 (a)). Interestingly, adenocarcinomas of neuroendocrine origin (NET) exhibit a differential expression profile, namely a decrease in LMP7 and absent LMP2 subunits. Additionally, LMP7 expression in PC and adjacent normal tissue in TRAMP prostates was verified by immunohistochemistry (IHC) staining (Figure 1(b)). LMP7 was highly expressed in luminal cells in PINs of prostate ventral (V) and dorsal lobes (DL), similar to the sites of highest probasin promotor-driven transgene levels.[24] In NET, we only found dim positivity for LMP7 in the periphery of tumor tissue – in agreement with our Western Blot results. Interestingly, high LMP7 expression was also detected in tumor-infiltrating cells. To test a potential anti-tumor activity of ONX 0914 against PC, we first induced immunoproteasome inhibition by IFNγ treatment in mouse and human cancer cell lines. Western Blot analysis of murine TRAMP-C2 cells and the human androgen-independent cell line DU145 treated with 300 nM ONX 0914 for 24 h shows irreversible inhibition of the LMP7 subunit indicated by the electrophoretic upward shifted bands to higher molecular weights (Figure 1(c)). Notably, the standard subunit PSMB5 was partially inhibited as well. LMP7 and LMP2 subunits are pivotal for maintaining the chymotrypsin-like activity of the immunoproteasome, which is of prime importance for degrading the bulk of protein substrates of the ubiquitin-proteasome system and proper protein homeostasis. Inhibition of the pro-teasomal protein degradation machinery leads to the accumulation of misfolded or deleterious proteins, which, if unresolved, triggers an acute proteotoxic stress response characterized by activation of the unfolded protein response (UPR), cessation of proliferation and might culminate in apoptotic cell death.[26] A hallmark of proteotoxicity is the accumulation of poly-ubiquitylated conjugates, which was prominent for ONX 0914 treated samples compared to DMSO control (Figure 1 (c)). In contrast to a less pronounced direct apoptotic effect by ONX 0914 on these cells, analyzed by Annexin V-PI staining (Figure 1(d)), cells became markedly more sensitive to ONX 0914 following pre-stimulation with IFNγ, suggesting that ONX 0914 could directly induce early (Fig. S1C) and late apoptotic events in prostate tumor cells surrounded by a pro-inflammatory microenvironment. Apoptotic cell death was further verified by increased cleavage of poly (ADP-ribose) polymerase (PARP) and activation of caspase 3 in ONX 0914 treated cells within the pro-inflammatory environment (Figure 1(d and e)). Thus, ONX 0914 induces apoptosis via activation of both intrinsic and extrinsic pathways. These results were unequivocally observed in the androgen-

independent cell line PC-3, as well as in LNCaP cells, which represent androgen-sensitive PC before androgen deprivation therapy (ADT) (Fig. S1).

Treatment with the selective immunoproteasome inhibitor ONX 0914 suppresses the formation of prostate cancer in TRAMP mice

To test the antitumor efficacy of ONX 0914 *in vivo*, we used the clinically relevant TRAMP mouse model which has been extensively used primarily due to pathologic features resembling human PC carcinogenesis. Male TRAMP mice express SV40 large and small T oncoproteins in secretory cells of the prostate epithelium under the control of the androgen-regulated pro-basin promoter.[22] T antigens abrogate tumor suppressor function which results in spontaneous progression of PC in the genetic background of C57BL/6 mice. Initial hyperplasia leads to generation of prostatic intraepithelial neoplasia (PIN) during weeks 10–16 and progresses to advanced adenocarcinoma in dorsal and lateral lobes by app. 18–24 weeks. By 28 weeks of age, most TRAMP mice have developed poorly differentiated carcinomas with metastatic dissemination of tumor cells to distant organs.[27] TRAMP mice were s.c. treated with 10 mg/kg ONX 0914 or vehicle control 3 times a week beginning at 10 weeks of age for long-term therapy of 22 weeks (Figure 2 (a)). At necropsy, the genitourinary tract (GU) weight (Figure 2(c)) and relative GU weight, calculated as (GU weight/body weight) × 100 (Fig. S2A) was used to evaluate the effect of immunoproteasome inhibition on PC progression. The average GU weight was significantly less after ONX 0914 therapy than in vehicle treated TRAMP mice, which commonly show enlargement and discoloration of the prostate tissue (Figure 2(b)). Additionally, treatment with the inhibitor shows extended survival compared to vehicle treated mice (Figure 2(d)).

In accordance with the macroscopically visible prominent decrease in tumor weight, histopathological analysis of prostate tissues supported the tumor reduction in ONX 0914 treated mice, as illustrated in Figure 2(e). TRAMP mice treated with the inhibitor developed lower incidences of dysplastic regions compared to vehicle control. Vehicle treated TRAMP mice show a prevalence of high-grade dysplasia, characterized by hyperplastic stratification of luminal epithelium with cribriform pattern and cellular atypia and high-grade PINs (HGPIN) with highly dysplastic luminal epithelium. The majority of lesions in ONX 0914 treated mice were characterized by epithelial stratification typical for low-grade PIN (LGPIN) or luminal epithelial hyperplasia without cellular atypia with a higher incidence of healthy glandular tissue and only rare occasional appearance of carcinoma *in situ*. Adenocarcinomas in vehicle treated mice were moderately to poorly differentiated, with widespread invasion of epithelial tumor cells into hypertrophied stroma, as well as large sections of complete disruption of glandular structural organization, while the incidence of adenocarcinomas was largely diminished with immunoproteasome inhibition.

TUNEL staining revealed a higher number of apoptotic cells in ONX 0914-treated prostate tumor tissue, especially in central areas of tumor glands compared to low TUNEL-positive
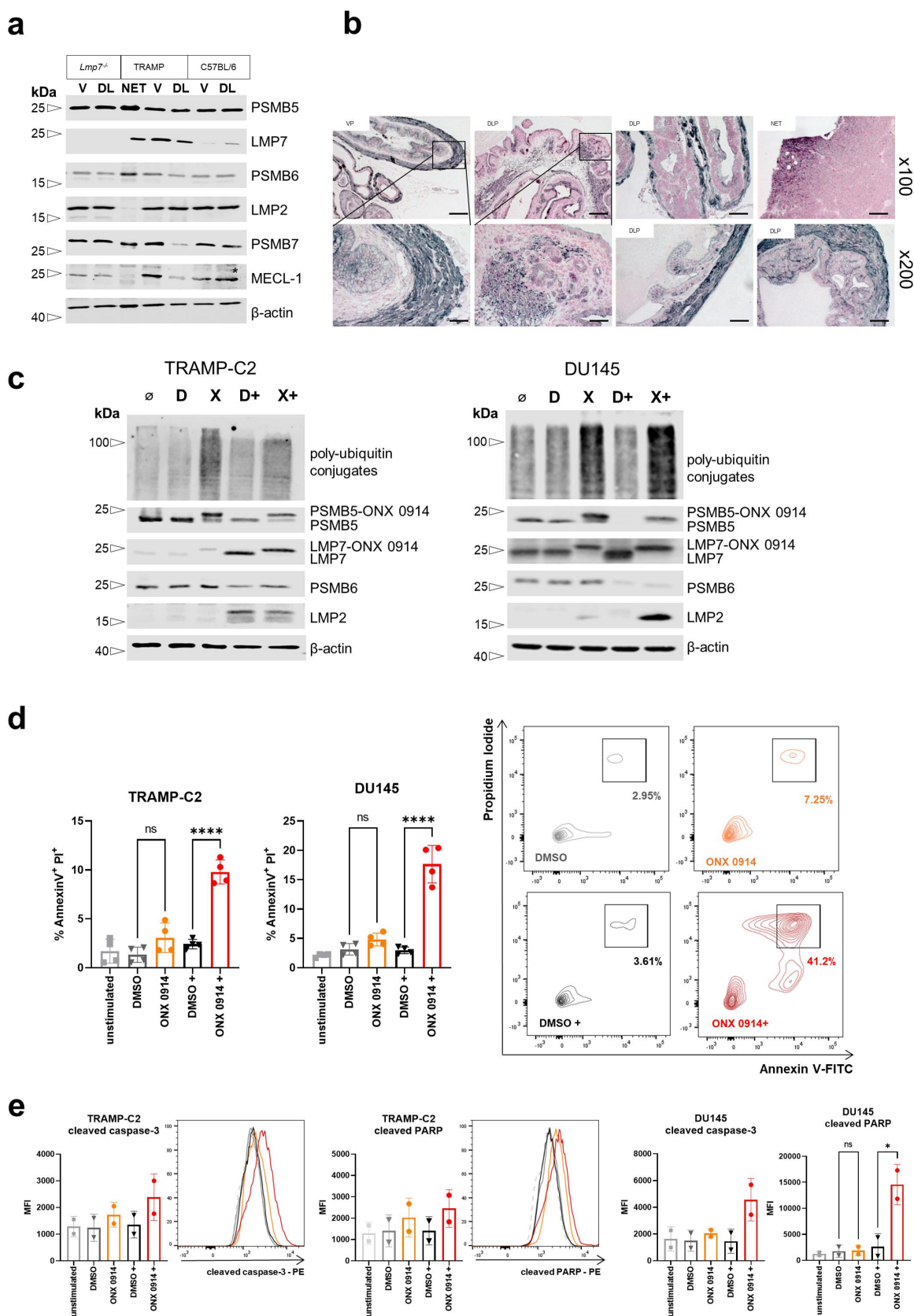
Figure 1. Inhibition of the immunoproteasome interferes with proteostasis and induces apoptosis in human and murine prostate cancer cells. (a) Western blot analysis of standard proteasome (PSMB5, PSMB6, PSMB7) and immunoproteasome (LMP7, LMP2, MECL-1) subunits in healthy prostate tissue and prostate tissue from tumor-bearing TRAMP mice. The expression of individual subunits was analyzed in ventral (VP) and dorsolateral (DL) prostate tissue of $Lmp7^{-/-}$ mice, TRAMP mice and C57BL/6 mice. The asterisk indicates high exposure to detect positive signals. Tissue from $Lmp7^{-/-}$ mice was used as negative control for the expression of LMP7. Relative levels of immunoproteasome subunits were decreased in poorly differentiated primary, neuroendocrine tumors (NET) of TRAMP mice. (b) Immunohistochemistry for LMP7 (black staining) in ventral and dorsolateral prostate lobes of TRAMP mice at 32 weeks. Note the decreased staining in NET tumor tissue. Scale bars: 200 μm for x100 original magnification, 100 μm for x200 original magnification. (c) Murine TRAMP-C2 cells or human DU145 cells were pre-treated with 200 U/mL IFNγ for 48 h (+), without pre-treatment or left untreated (∅). Western blot analysis of ubiquitin conjugate accumulation using anti-FK2 antibody and

staining in prostates of vehicle treated mice (Figure 2(e)), suggesting increased and long-term pro-apoptotic effects by treatment with the inhibitor. Furthermore, we analyzed the expression of the pro-inflammatory cytokine IL-17 in prostate tissue, since IL-17 is a major pro-tumorigenic factor in the prostate, thus playing an important role in development of prostatic inflammation and PC. ONX 0914 treatment led to significantly decreased IL-17 expression levels compared to vehicle control mice. There was a slight difference observed for IFNγ expression, which was moderately stronger in prostate tissue of inhibitor-treated mice (Fig. S2B). Notably, Gr1 positive lesions were barely detectable in ONX 0914-treated mice, demonstrating diminished infiltration of cells positive for the myeloid suppressor marker. In response to recent reports of extended MDSC infiltration in mouse and human PC tissue,[9,28] we analyzed the frequency of MDSC in prostate tissues of inhibitor- and vehicle-treated mice by flow cytometry. As illustrated in Figure 2(f), a decrease in total MDSC percentage was observed (left panel). MDSC are broadly subtyped into monocytic (M-MDSC) and polymorphonuclear MDSC (PMN-MDSC) based on differential expression of the cell surfer markers Ly6C and Ly6G. Both MDSC subtypes appear to have distinct roles in PC although their relative contribution still needs to be elucidated. The frequency of both MDSC subsets, as well as of TAMs (Fig. S2C) were significantly decreased in response to treatment with the inhibitor in contrast to vehicle treated mice.

Collectively, these data demonstrate inhibitory effects on progression of prostatic malignant lesions *in vivo* by inhibition of the immunoproteasome most likely via altering the pro-inflammatory and immunosuppressive tumor microenvironment.

ONX 0914 efficiently targets myeloid-derived suppressor cells and tumor-associated macrophages as potential antitumor targets

Besides MDSC, infiltration of inflammatory myeloid-derived cells such as M2-like, tumor-associated macrophages has been shown to correlate with PC aggressiveness and castration resistance.[29,30] To analyze direct effects of ONX 0914 on those two key players of PC carcinogenesis, mouse BM-derived monocytes were *in vitro* differentiated into MDSC and TAMs using GM-CSF and IL-6 or M-CSF. These cells were positively identified by the classical MDSC markers Gr1 and Ly6C/Ly6G, and F480+/Ly6G- for TAMs (Fig. S3A). MDSC as well as TAMs highly expressed immunoproteasome subunits, while subunits of the standard proteasome were also

detectable (Figure 3(a)). 24-hour treatment with the inhibitor eminently induced accumulation of ubiquitin conjugates as well as increased early (Fig. S3B) and late pro-apoptotic effects (Figure 3(b)), as assessed by Annexin V/PI staining. Similar to murine TRAMP-C2 cells and the human cell line DU145 (Figure 1), MDSC and TAMs treated with 300 nM ONX 0914 for 24 h show irreversible inhibition of the LMP7 subunit indicated by the electrophoretic upward shifted bands to higher molecular weights as we have previously observed. Notably, the standard subunit PSMB5 was partially inhibited as well. Whether the observed electrophoretic shift is indeed due to covalent binding of ONX 0914 or caused by another modification cannot be definitively determined. Interestingly, PSMB5 and PSMB6 are strongly up-regulated after ONX 0914 treatment. MDSC mediated immunosuppression partially relies on arginase to deplete L-arginine. We found reduced expression of arginase 1 in inhibitor-treated MDSC suggesting a reduction of immunosuppressive activity of these cells (Fig. S3C).

Inhibition of the immunoproteasome is also efficacious in therapeutic treatment of TRAMP prostate cancer

To assess the therapeutic potential of LMP7 inhibition, we treated TRAMP mice beginning at 26 weeks of age, when precancerous lesions already have established (Figure 4(a)). Prostate tumors of inhibitor treated mice were considerably smaller than those of the vehicle group at 32 weeks of age (Figure 4(b)). Also at later stages, ONX 0914 treatment led to a significant decrease in prostate carcinogenesis, as revealed by the analysis of GU weights (Figures 4(c), S4A) and improved overall survival (Figure 4d). ONX 0914 could effectively reduce PC progression, which was demonstrated by diminished lesions of HGPIN and rare occurrence of malignant adenocarcinoma formation (Figure 4(e)). Furthermore, inhibitor-treated mice showed significantly decreased incidences of distant metastasis, demonstrated by absent liver or pulmonary metastasis (Figure 4(e)). Additionally, more apoptotic cells were detectable after ONX 0914 treatment (Fig. S4C) compared to vehicle control. Similar to data obtained from the protective tumor setting, the density of IL-17 positive cells was diminished by treatment with the immunoproteasome inhibitor, while IFNγ expression was more intense (Fig. S4C). IHC staining for Gr1 also revealed a reduction of myeloid cells in the ONX 0914 group. Consistently, the prevalence of MDSC (Figure 4(f)) and to a lesser extent TAMs (Fig. S4B) in prostate tumor tissues was reduced after inhibitor therapy, however, not as prominent as after long-term ONX 0914 treatment.

---

analysis of standard proteasome (PSMB5, PSMB6, PSMB7) and immunoproteasome (LMP7, LMP2, MECL-1) subunits in response to treatment with 300 nM ONX (X, X+) or 0.3% DMSO (D, D+) for 24 hours. β-actin served as loading control. (d) Flow cytometric analysis of Annexin V/Propidium Iodide (PI) staining after 24 h of incubation with either 300 nM ONX 0914 or vehicle (0.3% DMSO) without or with IFNγ pretreatment (DMSO +, ONX 0914 +). Graphs indicate the percentage of Annexin V/PI – double positive cells. Representative density plots of gated Annexin V+ PI+ ONX 0914 or DMSO treated DU145 cells are shown in group-specific color code on the right. (e) The apoptotic markers active caspase-3 and cleaved PARP were analyzed by flow cytometry and are presented as MFI (mean fluorescence intensity). Cells were treated as described above. Representative histograms of TRAMP-C2 cells are shown on the right in group-respective color code. Data are presented as means ± SD from 3 independent experiments. Statistical significance was analyzed by ordinary one-way ANOVA. *P < .05, ****P < .0001; ns, not significant. NET, neuroendocrine tumors; V, ventral prostate; DL, dorsolateral prostate; D, DMSO; X, ONX 0914.
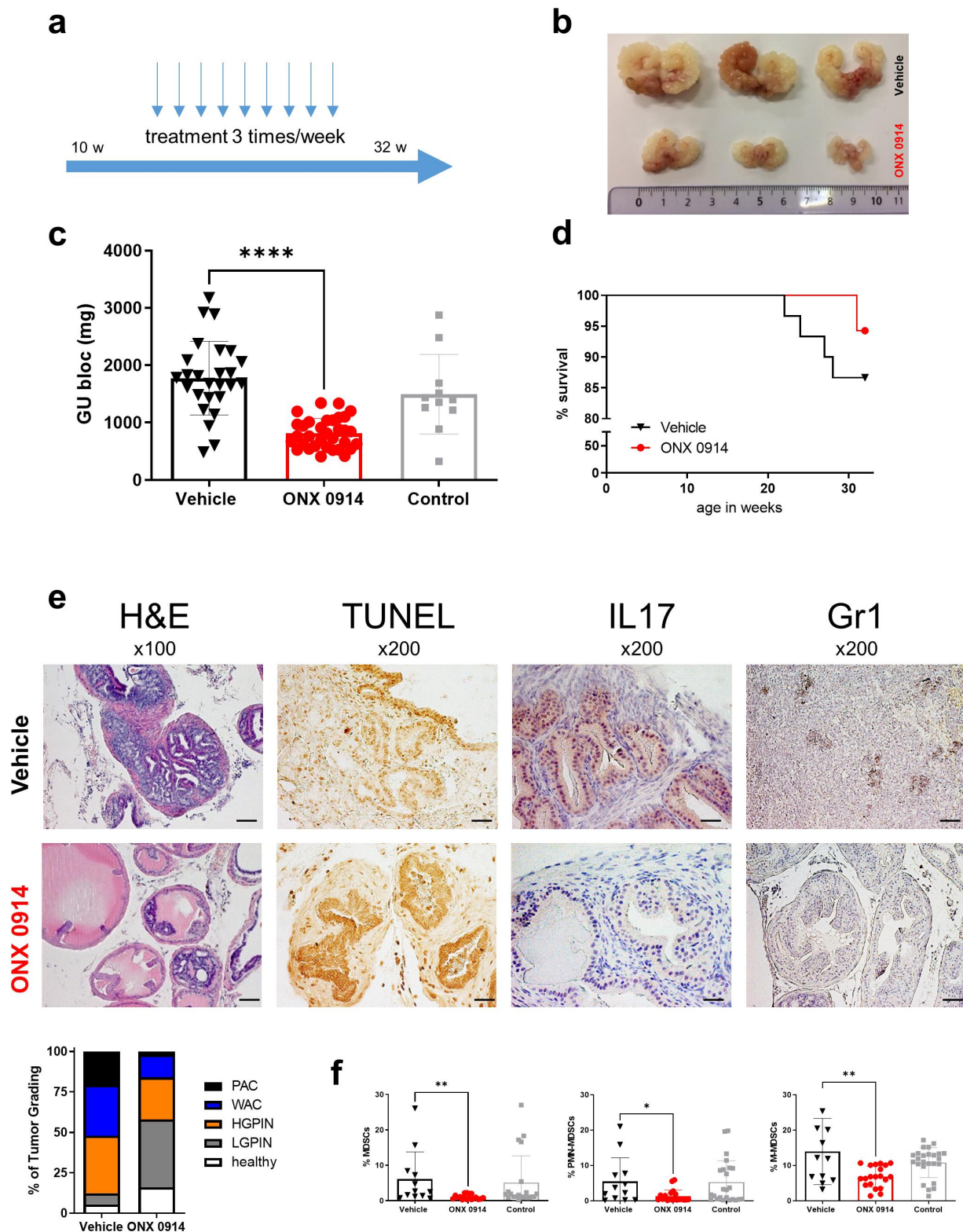
Figure 2. The *in vivo* anti-tumor effects of the immunoproteasome inhibitor ONX 0914 in TRAMP mice.

Thus, control of the immunosuppressive TME by ONX 0914 to induce anti-tumor responses and to reduce prostate tumor growth was also achievable at later stages of PC development.

Prostate carcinoma with neuroendocrine differentiation (NET) were eliminated from the analysis since these tumors originate independently from atypical hyperplasia and appeared in an uncontrollable manner before the designated endpoints. NET tumors, characterized by synaptophysin expression (Fig. S4F) are aggressive, poorly differentiated GU tumors involving different prostate lobes with weights ranging up to 12 g. Neuroendocrine prostate tumors are relatively
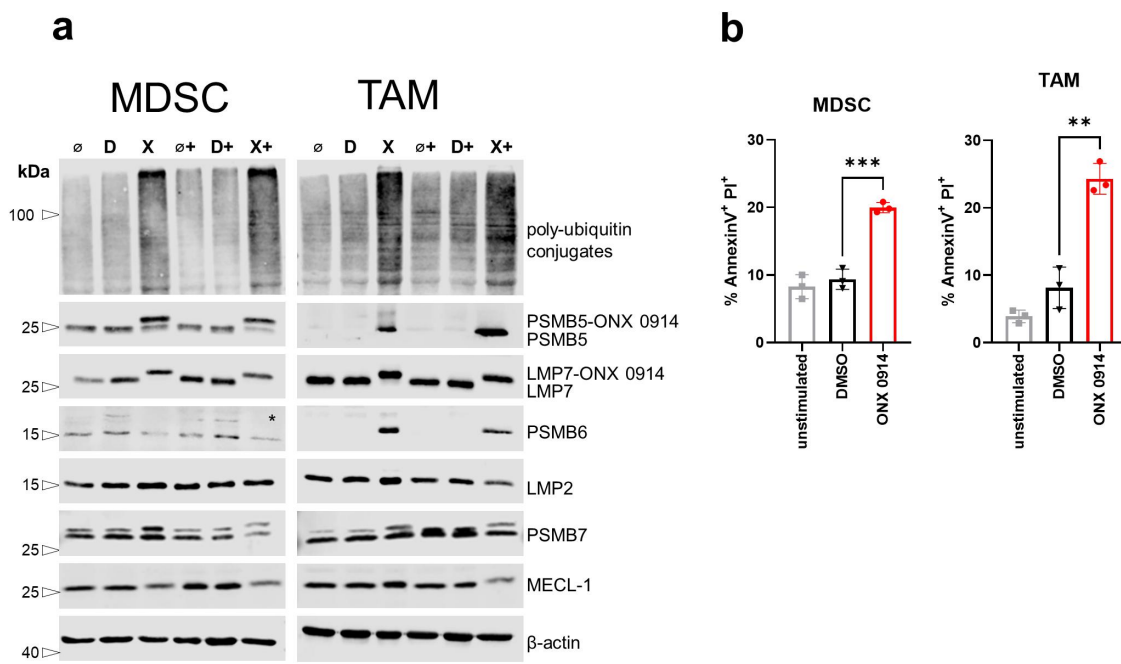
a

b

Figure 3. Immunoproteasome inhibitor ONX 0914 induces poly-ubiquitin accumulation and cell death in *in vitro* generated MDSC and TAMs.

uncommon in humans with only 10% of all cases. Nevertheless, LMP7 expression in NET suggests potential direct targeting by ONX 0914 (Fig. S4F). The analyzed large abdominal tumors were neither different in size nor quantity between the two treatment groups (Fig. S4D). However, tumor cell differentiation to the neuroendocrine phenotype was more associated with vehicle treated mice. NET tissue in ONX 0914-treated animals still exhibit gland architecture compared to poorly differentiated tumor in vehicle-treated mice, characterized by large cells with high nuclear to cytoplasmic ratio and anaplastic morphology. However, inhibitor treatment led to moderate reduction in IL-17 and Gr1 positivity, with more intense staining for IFNγ and apoptosis in NETs from the ONX 0914 group (Fig. S4E). The absence of targetable immune cells could explain the less beneficial effects of ONX 0914, however, the exact mechanisms have to be further elucidated.

Immunoproteasome inhibition shows therapeutic efficacy in castration-resistant prostate cancer

TRAMP tumorigenesis early develops androgen-independence, thus being an ideal model for human hormone-refractory PC. Almost all TRAMP mice develop neuroendocrine carcinomas post castration.[27,31,32] To investigate anti-tumorigenic efficacy of ONX 0914 for treatment of androgen-independent PC, we analyzed the effect of immunoproteasome inhibition post castration. Male TRAMP mice were surgically castrated at 24 weeks of age. Four weeks after castration, ONX 0914 or vehicle was injected every other day and analyzed by necropsy 22 weeks later (Figure 5 (a)). At sacrifice, most castrated TRAMP mice of the ONX 0914 group appeared without gross primary or metastatic tumors. Mice only developed hypoplastic tissue which lacked histological evidence of primary prostate tumor tissues, suggesting ONX 0914 prolongs cancer prevention in castrated individuals (Figure 5(b)). In contrast, a relevant fraction of the castrated mice of the vehicle

group developed tumors of neuroendocrine phenotype of high-grade, poorly differentiated prostate carcinoma cells (Figure 5(d)). Four out of ten mice in the vehicle cohort exhibited prostate tumors with foci of HGPIN and moderately differentiated adenocarcinomas. In contrast to ONX 0914 treated mice, all animals from the vehicle treated group exhibited macroscopic metastasis in lungs and livers identified by necropsy and microscopic analysis (Figure 5(e)). TUNEL positive cells were only scarcely detectable in both groups. Prostate tissues were further stained for the neuroendocrine marker synaptophysin, which was barely detectable in tissues of ONX 0914 treated mice. Positive focal staining was observed in prostate glands of vehicle treated mice (Figure 5(f)), as well as in macro-metastasis of lung and liver in both treatment groups. Similarly, the IL-17 or Gr1-positive prostate lesions were almost absent after immunoproteasome inhibition. Interestingly, ONX 0914 treatment might also influence metabolism and/or weight gain, since animals show reduced body weight and overall greater fitness compared to castrated mice of the vehicle group (Figure 5(c)). Tumor recurrence after therapy with prostatectomy or palliative ADT, is concomitant with formation of distant metastases. We found that primary tumors in CRPC-TRAMP mice showed a significant response to ONX 0914, however, in 2 out of 7 mice the therapeutic effect was not sustained and metastatic relapse of neuroendocrine phenotype occurred at distant sites, mainly in liver and lung (Fig. S5). Albeit the induction of apoptosis was detected in micrometastases in response to ONX 0914 compared to vehicle-treated CRPC-TRAMP mice. In summary, ONX 0914 treatment of TRAMP mice subjected to androgen deprivation therapy by surgical castration, largely reduced the frequency of recurrent PC.

Discussion

Immunoproteasome inhibitors suppress the development and progression of autoimmune diseases in numerous preclinical
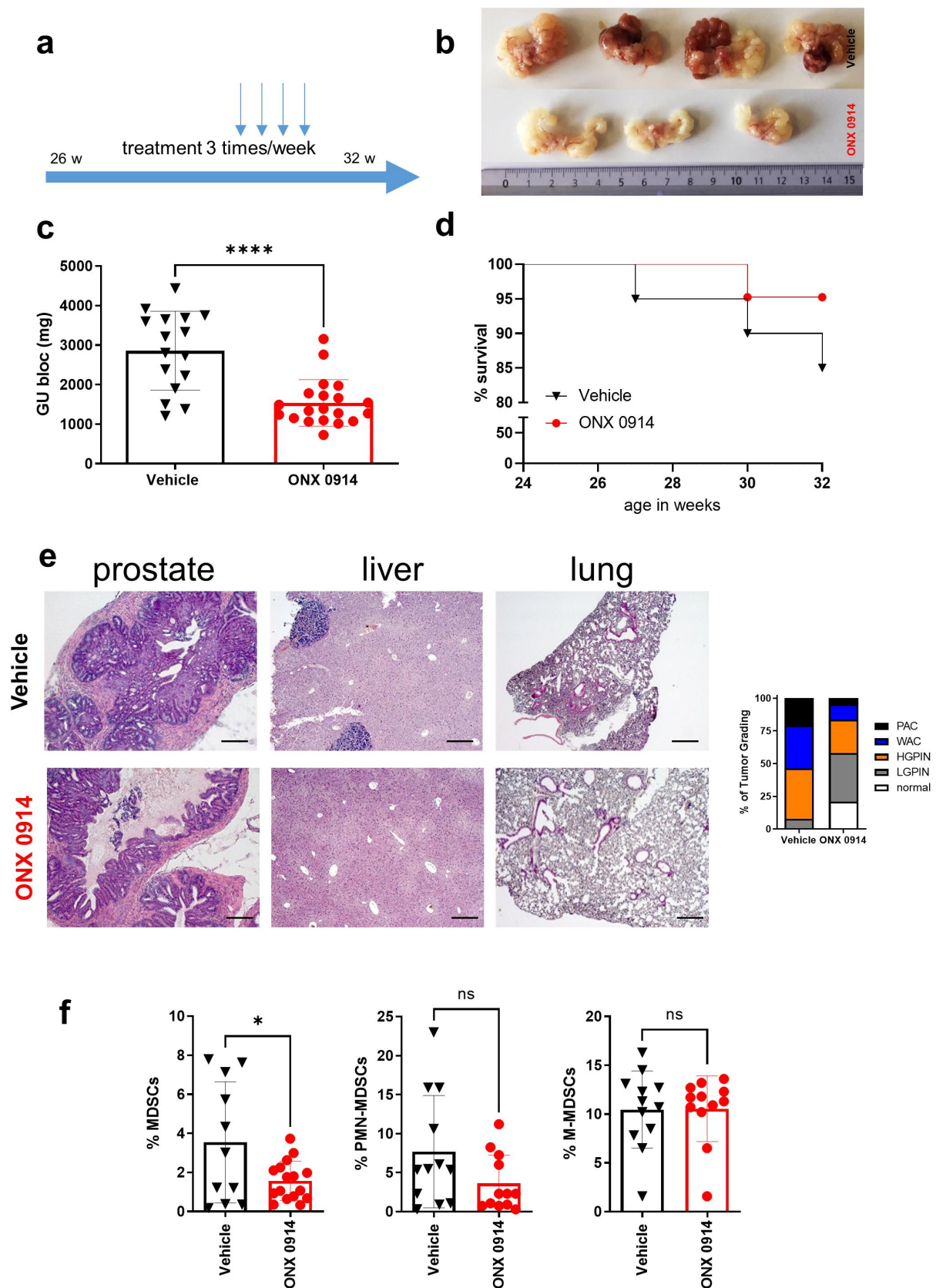
Figure 4. Therapeutic efficacy of ONX 0914 treatment in the autochthonous TRAMP mouse model.

mouse models and are currently investigated in phase II trials of autoimmune diseases.[33,34] Given that chronic inflammation is a risk factor for cancer development, we and others have previously investigated whether immunoproteasome inhibition can

also suppress the development and progression of colon cancer that is known to be promoted by inflammatory cytokines which are suppressed by immunoproteasome inhibition in autoimmune diseases. In fact, immunoproteasome inhibition with ONX 0914
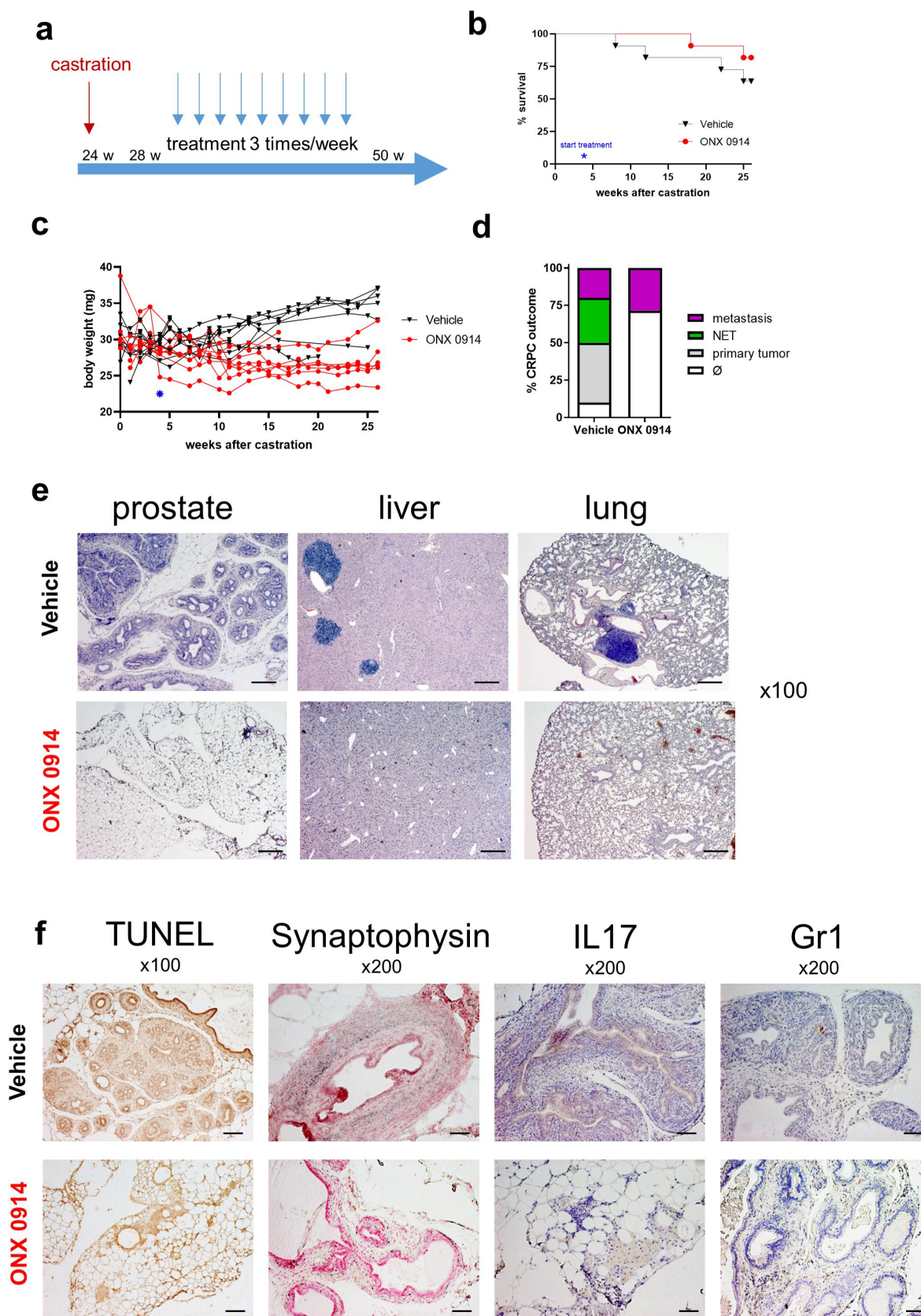
Figure 5. **Immunoproteasome inhibitor ONX 0914 inhibits adenocarcinoma and CRPC formation in castrated TRAMP mice.**(a) Experimental time schedule. Male TRAMP mice were castrated at 24 weeks of age and treated with ONX 0914 (10 mg/kg, s.c.; n = 8) or vehicle control (n = 10), starting 4 weeks post castration. Mice were sacrificed at 50 weeks of age for a total of 22 weeks of therapy. (b) Kaplan-Meier survival curve at the designated study point showing improved overall survival in ONX 0914 treated CRPC mice. A blue asterisk represents start of inhibitor treatment. (c) Body weight measurements of ONX 0914 and vehicle treated mice over time demonstrating increasing body weight levels in vehicle treated castrated animals. A blue asterisk represents start of inhibitor treatment. (d) Quantitation of pathological and clinical outcome of CRPC in all castrated TRAMP mice. (e) Representative H&E images of prostate tissues, lungs and livers of castrated TRAMP mice from both treatment groups. Scale bars represent 200 μm for original magnification x100; NET, neuroendocrine tumor. (f) TUNEL staining for detection of apoptosis (brown staining). Immunohistochemistry for synaptophysin (black staining), IL-17 and Gr1 (right panel, red staining). Scale bars: 200 μm for x100 original magnification, 100 μm for x200 original magnification.

markedly slowed down colon carcinoma progression in genetic and mutagen-induced models in therapeutic settings.[17,18] These results encouraged us to investigate a potential therapeutic effect of ONX 0914 in TRAMP mice building on the insight that PC progression is promoted by the same pro-inflammatory cytokines IL-6, TNF, IL-17, and IL-23.[9,19]

It has been shown that proteasome inhibitors enhance anti-proliferative, pro-apoptotic, anti-tumor and anti-angiogenic effects. The anti-tumor potential of proteasome inhibitors alone or in combination with other chemotherapeutic agents has been reported for PC cell lines.[35,36] In addition, a phase I clinical trial with the first-generation proteasome inhibitor bortezomib (PS-341, Velcade®) demonstrated anti-tumor activities for androgen-independent PC with accompanied downregulation of pro-inflammatory cytokines such as IL-17.[37] In fact, the immunoproteasome has recently gained more recognition as a potential therapeutic drug target to improve current anti-cancer therapies as it is selectively expressed in cells of the immune system and inflamed tissues, regulating pivotal pathways that are involved in tumor development and progression. Selective inhibition of the immunoproteasome using the irreversible epoxyketone inhibitor UK-101 was shown to induce cell cycle arrest and apoptosis in PC3 tumor cells, as well as reduced tumor growth in xenografted mice,[38] however, at concentrations highly exceeding the doses of immunoproteasome inhibitors used in this study which preserve immunoproteasome selectivity. The importance of the immunoproteasome in regulation of prostatic tumorigenesis is further highlighted by the fact that activity of immunoproteasomes is generally up-regulated in cancer cells after being exposed to an inflamed microenvironment. Additionally, inflamed mouse and human tissue show increased expression levels of immunoproteasome subunits probably induced by release of the pro-inflammatory cytokines TNF or IFNγ from infiltrating lymphocytes and monocytes already constitutively expressing immunoproteasomes.[39,40]

We have shown in this study that the expression of all three active site bearing immunoproteasome subunits LMP2, MECL-1, and LMP7 are prominently expressed in PC tissue from TRAMP mice and that these subunits are up-regulated in the murine TRAMP-tumor derived cell line TRAMP-C2 and the human PC lines DU-145 (Figure 1), PC3, and LNCaP (Fig. S1) upon stimulation with IFNγ. Treatment of these cell lines with ONX 0914 leads to a marked accumulation of poly-ubiquitin conjugates most likely because of a limitation of the overall proteasomal capacity. Such a disturbance of proteostasis is known to lead to the activation of the unfolded protein response and the induction of apoptosis.[26,41] Consistently, we have observed apoptosis induction in IFNγ treated but not untreated PC cell lines upon immunoproteasome inhibition as evidenced by PI/Annexin V stainings and enhanced levels of cleaved caspase 3 and PARP-1 (Figures 1, S1). It is therefore very likely that immunoproteasome inhibition in inflamed PC tumors exerts a direct cytocidal effect on PC cells due to induction of proteostasis failure.

The immunosuppressive myeloid derived cell types MDSC and TAMs which are both significantly increased in PC tissues, play a crucial role in the development of the inflammatory TME in PC, thereby cooperatively inhibiting effective anti-tumor immunity by immunosuppression and induction of regulatory T cells (Tregs). Thus, PC is considered to be an immunologically 'cold'

tumor.[7,9,19,29] Those cells are actively recruited to the tumor niche by IL-6 and several chemokines during PC progression.[29] It was reported, that especially MDSC are infiltrating into CRPC tissue compared to castration-sensitive prostate TME.[9] A higher MDSC density correlates with increased circulating IL-6 and confers development of metastatic PC and a worse overall survival.[42–44] MDSC mediate immunosuppression through a variety of mechanisms, including the release of reactive oxygen and nitrogen species, arginase I production or upregulation of PD-1 or M2 TAM polarization via IL-10.[45,46] Furthermore, MDSC promote PC progression by secretion of IL-23, the inducer of CRPC.[9] Thus, targeting MDSC is a promising therapeutic approach. We show that ONX 0914 treatment significantly reduces MDSC and TAM levels in the TME (Figure 2(e),(f); Figure 4(f)), potentially by direct apoptosis induction (Figure 3(b)) which leads to interception of the immunosuppressive effector functions. Several anti-inflammatory approaches focus on MDSC and TAM as prime therapeutic targets in PC, demonstrated by a variety of clinical trials targeting those subsets in PC patients. CSF-1 receptor antagonism or CXCR2 blockade resulted in decreased MDSC infiltration or alleviation of immunosuppressive activities,[7,9] while MDSC depletion with anti-Gr1 neutralizing antibodies sensitized prostate tumors to immune checkpoint therapy.[47] Inhibition of MDSC effector function by IL-23 blockade or by suppressing JAK/STAT3 signaling restored androgen deprivation sensitivity and showed therapeutic efficacy in conditional Pten knockout mouse models and induction of anti-tumor immune response in human PC patients.[9] Recently, we could show that ONX 0914 leads to reduced IL-23 secretion by selective killing of human monocytes,[15] which strongly resembles the active targeting of MDSC present in this study. Other anti-inflammatory agents, such as non-steroidal anti-inflammatory drugs have also been tested in PC immunotherapy. For example, the COX2 inhibitor celecoxib could reduce prostate tumor growth in TRAMP mice.[48] Furthermore, celecoxib treatment of Pten-deficient mice suppressed M2 TAM and MDSC infiltration and effector function.[49]

We also observed reduction of IL-17 expression in ONX 0914 treated prostate tumors (Figures 2(e), S4C). Several studies have demonstrated that IL-17 promotes the development of PC by increased proliferation, decreased apoptosis and enhanced angiogenesis in several animal models of autochthonous cancer. Furthermore, IL-17 recruits myeloid-derived suppressor cells into the tumor niche. IL-17 also leads to increased immunosuppressive function of MDSC on T cells, thereby creating an immunotolerant TME.[50] Collectively, it was shown that ONX 0914 regulates the production of key players of PC development, namely IL-6, IL-17, and IL-23. The results of this study corroborate the anti-inflammatory action of ONX 0914 which is most likely instrumental for combatting PC and CRPC.

As shown in Figure 1(a), neuroendocrine tumor tissue barely express immunoproteasome subunits pointing that the immunoproteasome inhibitor might not act directly on those malignant cells. Neuroendocrine (NE) prostate carcinoma is a very aggressive prostate cancer subtype and may develop in 10–20% of CRPC patients as cause of prolonged androgen-deprivation therapy.[51] Currently, there are no treatment options for this aggressive treatment-related prostate cancer subtype. We hypothesize that the conversion of the immunosuppressive TME by ONX 0914 treatment might also be beneficial for NE-like CRPC. Suppression of

Th17 differentiation and reduced IL-17 production in response to treatment with the immunoproteasome inhibitor ONX 0914 has already been shown in several models of autoimmune disease and inflammation-associated tumor models.[13,14,16,17] Besides its pro-tumorigenic function in PC,[3] IL-17 has also been testified to promote castration-resistant prostate cancer development and neuroendocrine differentiation by promotion of angiogenesis and induction of epithelial–mesenchymal transition (EMT).[52] ONX 0914 treatment might partly counteract IL-17-induced EMT and regulate neuroendocrine prostate cancer progression by inhibition of EMT. By subversion of the immunosuppressive IL-17 phenotype, as well as ONX 0914-mediated reduction of intra-tumoral Gr-1+ myeloid cells, immunoproteasome inhibition might render NE-prostate tumor tissue more susceptible to tumor killing by increasing the density of IFNγ+ secreting cells. Due to the aggressive proliferative phenotype of neuroendocrine tumors, ONX 0914 mediated immunotherapy would benefit from combination treatments with anti-microtubule agents such as Docetaxel as one of the few FDA-approved targets for CRPC.[53]

In the present study, we show that immunoproteasome inhibition holds great promise for the treatment of PC. ONX 0914 treatment combines the benefits of anti-inflammatory and direct anti-oncogenic effects on PC and suppression of tumor relapse after castration with the potential of meeting a major medical need. Given that a close analogue of ONX 0914, namely the peptidomimetic epoxyketone inhibitor KZR-616,[34] is currently applied in phase II clinical trials for the therapy of autoimmune diseases, the benefit of treating PC patients with an immunoproteasome inhibitor can rapidly be investigated in clinical trials.

Acknowledgments

Author contributions

JK, DH, and JL designed and performed experiments and evaluated data. JK wrote the manuscript. FO and MB provided experimental help and technical advice with mouse work and histology and corrected the manuscript. MB corrected and refined the manuscript.

Disclosure statement

The authors report there are no competing interests to declare.

Funding

ORCID

Julia Koerner (iD) http://orcid.org/0000-0002-6964-4459
Dennis Horvath (iD) http://orcid.org/0000-0001-9310-536X
Franziska Oliveri (iD) http://orcid.org/0000-0002-3280-448X
Jun Li (iD) http://orcid.org/0000-0003-0891-4328
Michael Basler (iD) http://orcid.org/0000-0002-9428-2349

References

1. de Bono JS, Guo C, Gurel B, De Marzo AM, Sfanos KS, Mani RS, Gil J, Drake CG, Alimonti A. Prostate carcinogenesis: inflammatory storms. Nat Rev Cancer. 2020;20(8):455–469. doi:10.1038/s41568-020-0267-9.
2. Sfanos KS, Yegnasubramanian S, Nelson WG, De Marzo AM. The inflammatory microenvironment and microbiome in prostate cancer development. Nat Rev Urol. 2018;15:11–24.
3. Zhang Q, Liu S, Zhang Q, Xiong Z, Wang AR, Myers L, et al. Interleukin-17 promotes development of castration-resistant prostate cancer potentially through creating an immunotolerant and pro-angiogenic tumor microenvironment. Prostate. 2014;74:869–879.
4. Zhang Q, Liu S, Ge D, Cunningham DM, Huang F, Ma L, et al. Targeting Th17-IL-17 pathway in prevention of micro-invasive prostate cancer in a mouse model. Prostate. 2017;77:888–899.
5. Sfanos KS, Bruno TC, Maris CH, Xu L, Thoburn CJ, DeMarzo AM, et al. Phenotypic analysis of prostate-infiltrating lymphocytes reveals TH17 and Treg skewing. Clin Cancer Res: an Offl J Am Assoc Cancer Res. 2008;14:3254–3261.
6. Derhovanessian E, Adams V, Hahnel K, Groeger A, Pandha H, Ward S, et al. Pretreatment frequency of circulating IL-17+ CD4+ T-cells, but not Tregs, correlates with clinical response to whole-cell vaccination in prostate cancer patients. Int J Cancer. 2009;125:1372–1379.
7. Garcia AJ, Ruscetti M, Arenzana TL, Tran LM, Bianci-Frias D, Sybert E, et al. Pten null prostate epithelium promotes localized myeloid-derived suppressor cell expansion and immune suppression during tumor initiation and progression. Mol Cell Biol. 2014;34:2017–2028.
8. Lorente D, Mateo J, Templeton AJ, Zafeiriou Z, Bianchini D, Ferraldeschi R, et al. Baseline neutrophil-lymphocyte ratio (NLR) is associated with survival and response to treatment with second-line chemotherapy for advanced prostate cancer independent of baseline steroid use. Ann Oncol. 2015;26:750–755.
9. Calcinotto A, Spataro C, Zagato E, Di Mitri D, Gil V, Crespo M, et al. IL-23 secreted by myeloid cells drives castration-resistant prostate cancer. Nature. 2018;559:363–369.
10. Collins GA, Goldberg AL. The logic of the 26S proteasome. Cell. 2017;169:792–806.
11. Muchamuel T, Basler M, Aujay MA, Suzuki E, Kalim KW, Lauer C, et al. A selective inhibitor of the immunoproteasome subunit LMP7 blocks cytokine production and attenuates progression of experimental arthritis. Nat Med. 2009;15:781–787.
12. Groettrup M, Kirk CJ, Basler M. Proteasomes in immune cells: more than peptide producers? Nat Rev Immunol. 2010;10:72–77.
13. Basler M, Mundt S, Muchamuel T, Moll C, Jiang J, Groettrup M, et al. Inhibition of the immunoproteasome ameliorates experimental autoimmune encephalomyelitis. EMBO Mol Med. 2014;6:226–238.
14. Basler M, Dajee M, Moll C, Groettrup M, Kirk CJ. Prevention of experimental colitis by a selective inhibitor of the immunoproteasome. J Immunol. 2010;185:634–641.
15. Basler M, Claus M, Klawitter M, Goebel H, Groettrup M. Immunoproteasome inhibition selectively kills human CD14(+) monocytes and as a result dampens IL-23 secretion. J Immunol. 2019;203:1776–1785.
16. Basler M, Lindstrom MM, LaStant JJ, Bradshaw JM, Owens TD, Schmidt C, et al. Co-inhibition of immunoproteasome subunits LMP2 and LMP7 is required to block autoimmunity. EMBO Rep. 2018;19.
17. Koerner J, Brunner T, Groettrup M. Inhibition and deficiency of the immunoproteasome subunit LMP7 suppress the development and progression of colorectal carcinoma in mice. Oncotarget. 2017;8:50873–50888.

18. Vachharajani N, Joeris T, Luu M, Hartmann S, Pautz S, Jenike E, et al. Prevention of colitis-associated cancer by selective targeting of immunoproteasome subunit LMP7. Oncotarget. 2017;8: 50447–50459.

19. Li N, Grivennikov SI, Karin M. The unholy trinity: inflammation, cytokines, and STAT3 shape the cancer microenvironment. Cancer Cell. 2011;19:429–431.

20. Gingrich JR, Barrios RJ, Morton RA, Boyce BF, DeMayo FJ, Finegold MJ, et al. Metastatic prostate cancer in a transgenic mouse. Cancer Res. 1996;56:4096–4102.

21. Fehling HJ, Swat W, Laplace C, Kuehn R, Rajewsky K, Mueller U, et al. MHC class I expression in mice lacking proteasome subunit LMP-7. Science. 1994;265:1234–1237.

22. Greenberg NM, DeMayo F, Finegold MJ, Medina D, Tilley WD, Aspinall JO, et al. Prostate cancer in a transgenic mouse. Proc Natl Acad Sci U S A. 1995;92:3439–3443.

23. Lutz MB, Kukutsch N, Ogilvie AL, Rossner S, Koch F, Romani N, et al. An advanced culture method for generating large quantities of highly pure dendritic cells from mouse bone marrow. J Immunol Meth. 1999;223:77–92.

24. Berman-Booty LD, Sargeant AM, Rosol TJ, Rengel RC, Clinton SK, Chen CS, et al. A review of the existing grading schemes and a proposal for a modified grading scheme for prostatic lesions in TRAMP mice. Toxicol Pathol. 2012;40:5–17.

25. Wikström P, Lindahl C, Bergh A. Characterization of the auto-chthonous transgenic adenocarcinoma of the mouse prostate (TRAMP) as a model to study effects of castration therapy. Prostate. 2005;62:148–164.

26. Li J, Koerner J, Basler M, Brunner T, Kirk CJ, Groettrup M. Immunoproteasome inhibition induces plasma cell apoptosis and preserves kidney allografts by activating the unfolded protein response and suppressing plasma cell survival factors. Kidney Int. 2019;95:611–623.

27. Kaplan-Lefko PJ, Chen TM, Ittmann MM, Barrios RJ, Ayala GE, Huss WJ, et al. Pathobiology of autochthonous prostate cancer in a pre-clinical transgenic mouse model. Prostate. 2003;55:219–237.

28. Hossain DM, Pal SK, Moreira D, Duttagupta P, Zhang Q, Won H, et al. TLR9-targeted STAT3 silencing abrogates immunosuppres-sive activity of myeloid-derived suppressor cells from prostate cancer patients. Clin Cancer Res: an Offl J Am Assoc Cancer Res. 2015;21:3771–3782.

29. Comito G, Giannoni E, Segura CP, Barcellos-de-Souza P, Raspollini MR, Baroni G, et al. Cancer-associated fibroblasts and M2-polarized macrophages synergize during prostate carcinoma progression. Oncogene. 2014;33:2423–2431.

30. Nonomura N, Takayama H, Nakayama M, Nakai Y, Kawashima A, Mukai M, et al. Infiltration of tumour-associated macrophages in prostate biopsy specimens is predictive of disease progression after hormonal therapy for prostate cancer. BJU Int. 2011;107:1918–1922.

31. Gingrich JR, Barrios RJ, Kattan MW, Nahm HS, Finegold MJ, Greenberg NM. Androgen-independent prostate cancer pro-gression in the TRAMP model. Cancer Res. 1997;57:4687–4691.

32. Chiaverotti T, Couto SS, Donjacour A, Mao JH, Nagase H, Cardiff RD, et al. Dissociation of epithelial and neuroendocrine carcinoma lineages in the transgenic adenocarcinoma of mouse prostate model of prostate cancer. Am J Pathol. 2008;172:236–246.

33. Basler M, Mundt S, Bitzer A, Schmidt C, Groettrup M. The immu-noproteasome: a novel drug target for autoimmune diseases. Clin Exp Rheumatol. 2015;33:S74–79.

34. Lickliter J, Anderl J, Kirk CJ, Wang J, Bomba D. KZR-616, a Selective Inhibitor of the Immunoproteasome, shows a promising safety and target inhibition profile in a phase I, double-blind, single (SAD) and multiple ascending dose (MAD) study in healthy volunteers arthritis rheumatol. 2017;Vol. 69 suppl 10:Abstract 2587.

35. Kuroda K, Liu H. The proteasome inhibitor, bortezomib, induces prostate cancer cell death by suppressing the expression of prostate-specific membrane antigen, as well as androgen receptor. Int JOncol. 2019;54:1357–1366.

36. Gopalakrishnan S, Ediga HH, Reddy SS, Reddy GB, Ismail A. Procyanidin-B2 enriched fraction of cinnamon acts as a proteasome inhibitor and anti-proliferative agent in human prostate cancer cells. IUBMB Life. 2018;70:445–457.

37. Papandreou CN, Daliani DD, Nix D, Yang H, Madden T, Wang X, et al. Phase I trial of the proteasome inhibitor bortezomib in patients with advanced solid tumors with observations in androgen-independent prostate cancer. J Clin Oncol. 2004;22: 2108–2121.

38. Wehenkel M, Ban JO, Ho YK, Carmony KC, Hong JT, Kim KB. A selective inhibitor of the immunoproteasome subunit LMP2 induces apoptosis in PC-3 cells and suppresses tumour growth in nude mice. Br J Cancer. 2012;107:53–62.

39. Visekruna A, Slavova N, Dullat S, Grone J, Kroesen AJ, Ritz JP, et al. Expression of catalytic proteasome subunits in the gut of patients with Crohn's disease. Int J Colorectal Dis. 2009;24: 1133–1139.

40. Kremer M, Henn A, Kolb C, Basler M, Moebius J, Guillaume B, et al. Reduced immunoproteasome formation and accumulation of immunoproteasomal precursors in the brains of lymphocytic chor-iomeningitis virus-infected mice. J Immunol. 2010;185:5549–5560.

41. Hetz C, Chevet E, Harding HP. Targeting the unfolded protein response in disease. Nat Rev Drug Discov. 2013;12:703–719.

42. Iea S. The level of myeloid derived-suppressor cells in peripheral blood of patients with prostate cancerafter various types of therapy. Pol J Pathol. 2020;71:46–54.

43. Santegoets SJ, Stam AG, Lougheed SM, Gall H, Jooss K, Sacks N, et al. Myeloid derived suppressor and dendritic cell subsets are related to clinical outcome in prostate cancer patients treated with prostate GVAX and ipilimumab. J Immunother Cancer. 2014;2:31.

44. Chi N, Tan Z, Ma K, Bao L, Yun Z. Increased circulating myeloid-derived suppressor cells correlate with cancer stages, interleukin-8 and −6 in prostate cancer. Int J Clin Exp Med. 2014;7:3181–3192.

45. Sanaei MJ, Salimzadeh L, Bagheri N. Crosstalk between myeloid-derived suppressor cells and the immune system in pros-tate cancer: mDSCs and immune system in Prostate cancer. J Leukocyte Biol. 2020;107:43–56.

46. Veglia F, Sanseviero E, Gabrilovich DI. Myeloid-derived suppres-sor cells in the era of increasing myeloid cell diversity. Nat Rev Immunol. 2021;21:485–498.

47. Lu X, Horner JW, Paul E, Shang X, Troncoso P, Deng P, et al. Effective combinatorial immunotherapy for castration-resistant prostate cancer. Nature. 2017;543:728–732.

48. Gupta S, Adhami VM, Subbarayan M, MacLennan GT, Lewin JS, Hafeli UO, et al. Suppression of prostate carcinogenesis by dietary supplementation of celecoxib in transgenic adenocarcinoma of the mouse prostate model. Cancer Res. 2004;64:3334–3343.

49. Hayashi T, Fujita K, Nojima S, Hayashi Y, Nakano K, Ishizuya Y, et al. High-fat diet-induced inflammation accelerates prostate can-cer growth via IL6 signaling. Clin Cancer Res. 2018;24:4309–4318.

50. He D, Li H, Yusuf N, Elmets CA, Li J, Mountz JD, et al. IL-17 promotes tumor development through the induction of tumor promoting microenvironments at tumor sites and myeloid-derived suppressor cells. J Immunol. 2010;184:2281–2288.

51. Abida W, Cyrta J, Heller G, Prandi D, Armenia J, Coleman I, Cieslik M, Benelli M, Robinson D, Van Allen EM, et al. Genomic correlates of clinical outcome in advanced prostate cancer. Proc. Natl. Acad. Sci. U. S. A. 2019;166:11428–11436.

52. Zhang Q, Liu S, Parajuli KR, Zhang W, Zhang K, Mo Z, Liu J, Chen Z, Yang S, Wang AR, et al. Interleukin-17 promotes prostate cancer via MMP7-induced epithelial-to-mesenchymal transition. Oncogene. 2017;36:687–699.

53. Tannock IF, de Wit R, Berry WR, Horti J, Pluzanska A, Chi KN, Oudard S, Théodore C, James ND, Turesson I, et al. Docetaxel plus prednisone or mitoxantrone plus prednisone for advanced prostate cancer. N. Engl. J. Med. 2004;351:1502–1512.